Trade-offs Between the Quality of Service, Computational Cost and Cooling Complexity in Interference-Dominated Multi-User SDMA Systems

Aslan, Yanki; Puskely, Jan; Roederer, Antoine; Yarovoy, Alexander

DOI
10.1049/iet-com.2019.0206

Publication date
2020

Document Version
Final published version

Published in
IET Communications

IET Communications

Research Article

IET Journals
The Institution of Engineering and Technology

Trade-offs between the quality of service, computational cost and cooling complexity in interference-dominated multi-user SDMA systems

ISSN 1751-8628
Received on 20th February 2019
Revised 4th September 2019
Accepted on 5th November 2019
E-First on 11th December 2019
doi: 10.1049/iet-com.2019.0206
www.ietdl.org

Yanki Aslan[1] ✉, Jan Puskely[1], Antoine Roederer[1], Alexander Yarovoy[1]

[1]*Department of Microelectronics, Microwave Sensing, Signals and Systems Group, Delft University of Technology, Delft, The Netherlands*

✉ *E-mail: Y.Aslan@tudelft.nl*

Abstract: The future fifth generation (5G) systems will aim to design low-cost phased array base station antenna systems at mm-waves for simultaneous multiple beamforming with enhanced spatial multiplexing, limited interference, acceptable power consumption, suitable processing complexity, and passive cooling. In this study, a multi-user space division multiple access (SDMA) model is developed to investigate the trade-off between the quality of service (QoS), computational complexity in beamforming and cooling requirements for various use cases, and a number of users. The QoS at the user ends is rated by assessing the statistical signal-to-interference-plus-noise ratios (SINRs). Two beamforming algorithms, namely conjugate beamforming (CB) and zero-forcing (ZF), are considered and compared. Depending on the deployment scenario, rotated and optimised array layouts are proposed to be used in CB with the least computational complexity while providing relatively good QoS. Different reduced-complexity ZF algorithms are introduced as a compromise between the SINR performance and computational burden. The impact of the number of simultaneously served users on the thermal management in active integrated 5G base station antenna arrays is investigated as well.

1 Introduction

The concept of space division multiple access (SDMA), which was first introduced in [1] and has been used in space applications for decades has recently regained attention with the development of mm-wave fifth generation (5G) technologies having demanding criteria on the channel capacity [2]. Using SDMA at the multi-beam 5G base station (BS) antennas, the system capacity of the communication network can be increased by re-using the same time-frequency resource in several different (and preferably well separated) beams. Furthermore, SDMA can be straightforwardly combined with the well-established code division multiple access technique to further enhance the capacity, especially for the users that are too close to each other and cannot be resolved by the antenna beam [3].

Multi-beam antenna synthesis and performance evaluation in 5G SDMA systems at mm-waves must combine different disciplines, including but not limited to signal processing, front-end circuitry design, channel propagation, and medium access control (MAC) aspects (see Fig. 1). Although separate comprehensive studies exist in each field (multiple beam antennas [4], beamforming algorithms [5], propagation models [6] etc.), the concept of inter-disciplinary work is relatively new in the antenna engineering community. Traditionally, array design has been performed based on satisfying the given criteria on the radiation patterns [gain, side-lobe levels (SLLs), beamwidth etc.] as in [7–9].

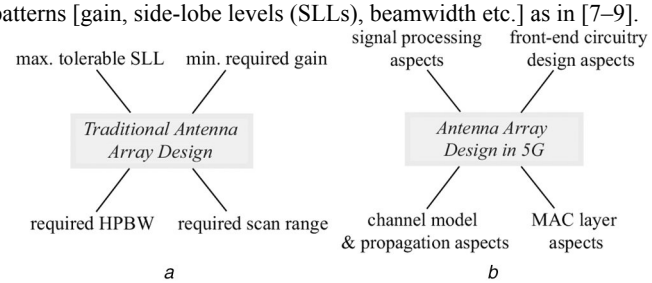

Fig. 1 *Design methodologies for antenna arrays*
(a) Traditional approach,
(b) 5G perspective

This study combines multiple disciplines in 5G SDMA by addressing all the aspects mentioned in Fig. 1*b*. A multi-user system model with a meaningful link budget is formulated considering line-of-sight (LoS) only propagation environments. Two different application scenarios are investigated considering either ground-only users or users/relays at different heights. An interference-aware user scheduling algorithm is proposed, which guarantees an almost-uniform power distribution across the array. Being the most power and computation efficient beamforming algorithm, conjugate beamforming (CB) is investigated with different array topologies. The performance of CB is compared with the complexity-reduced zero-forcing (ZF) algorithms that are able to strongly reduce or cancel out the inter-user interferences. Lastly, thermal simulations are performed to analyse the impact of the number of simultaneous co-frequency users on the transceiver chip temperature. A summary of the paper content with respect to each complementary research domain is given in Table 1.

Using the system model developed, the trade-off between the quality of service (QoS), computational cost, and complexity of thermal management are investigated at the 5G multi-beam BS antenna arrays. The statistical system QoS performance evaluation is given in terms of the cumulative distribution function (CDF) of signal-to-interference-plus-noise ratio (SINR), the computational cost is given in terms of floating point operations per second (FLOPS) and the cooling complexity is discussed via the computation of the maximum chip junction temperature in the array.

The major contributions of this study are listed as follows:

(C-i) A novel LoS SDMA system model that incorporates a 5G mm-wave link budget is proposed.
(C-ii) A novel and generalised classification of the 5G use cases (depending on the BS deployment scenario and user locations) is performed.
(C-iii) From the antenna radiation pattern perspective, an original and intuitive simultaneous, co-frequency user selection technique in SDMA is proposed.
(C-iv) The BS array rotation effect on the statistical user SINRs is investigated for the first time.

Table 1 Paper content with respect to the research topics

Research topic	Paper content
channel modelling and propagation	LoS SDMA system model and mm-wave link budget in different BS deployment scenarios
front-end circuitry design	power-efficient array synthesis and chip cooling
MAC	user selection and scheduling approaches
signal processing	several beamforming algorithms with/ without complexity reduction

Table 2 Recent publications in 5G antenna system design combining different disciplines

Complementary research domain	Ref. #
signal processing and beamforming algorithms	[10–14]
front-end circuitry design and efficiency	[15–21]
MAC protocols	[22–24]
channel modelling and propagation	[25–30]

(C-v) The optimised BS array layouts' statistical system performance is evaluated for the first time.
(C-vi) A novel reduced complexity ZF algorithm is introduced, which is based on a reference interference-to-noise-ratio (INR) threshold.
(C-vii) The relation between the complexity of thermal management and the number of simultaneously served users is investigated for the first time.
(C-viii) The pairwise trade-off between the QoS, computational burden and cooling complexity in 5G BS arrays is analysed for the first time, with useful insights and system design recommendations.

2 Related work

Some of the recent publications that combine antenna array synthesis with complementary research domains are provided in Table 2. Among the listed study areas, signal processing aspects consist of the study on linear, non-linear, narrowband, wideband, switched or adaptive beamforming algorithms. In this field, it is desired to achieve low computational complexity and high processing speed [10]. Some related works include the effect of total antenna number and radio frequency chains on the performance of code book-based or ZF-based beamforming [11–13] and combination of adaptive beamforming techniques with an antenna selection procedure [14].

Front-end circuitry design aspects are related to the power output and efficiency of the transceiver chips, heat dissipation, and cost. It is important to keep the amplifiers operating at the same, efficient working point [31] and ensure sufficient cooling of the beamforming chips at the integrated antennas [15]. In the past few years, several hybrid beamforming antenna array architectures have been proposed [16–18]. Power efficiency has been optimised using space-tapered arrays [19, 20]. Thermal problems due to the high heat dissipation of mm-wave chips have been eased by using fully-passive central processing unit (CPU) cooler heatsinks in combination with array topology optimisation [15] and highly conductive substrates [21].

MAC layer aspects cover the design of the medium access periods and rules when setting up an efficient link between the BS and users. It is essential to apply smart user selection and scheduling algorithms [22]. Some recent antenna-related works in this domain include the investigation of the effect of antenna beamwidth on the time spent for aligning the transmit and receive beams and the effect of small angle mismatches [23, 24].

Lastly, channel modelling and propagation aspects deal with deciding on the propagation parameters depending on the particular environment. When designing the BS antennas, the application scenario and BS antenna mounting location should be taken into account, together with a meaningful link-budget [32]. Some recent works on joint channel modelling and antenna synthesis include optimisation of array layouts depending on the statistical user throughput [25, 26], compact representation of propagation channels [27], investigation of a number of simultaneous BS antenna beams [28, 29] and user distributions and inter-user spacings [30].

To the best of the authors' knowledge, there is no prior work that jointly considers all the above-mentioned complementary research domains simultaneously. The presented study, on the other hand, combines different disciplines as previously stated in Table 1 and aims to highlight some of the system design trade-offs that will be faced when designing a complete 5G antenna array system.

The rest of the paper is organised as follows. Section 3 describes the system model. The use cases are presented in Section 4. The comparisons of QoS and computational complexity are given in Section 5 for different array topologies and beamforming techniques. The thermal simulation results are presented in Section 6 with a critical discussion on the challenge of array cooling. Section 7 concludes the paper.

3 System model

We consider an isolated cell sector in which a BS with M antenna elements is serving K single, omnidirectional antenna users in pure LoS simultaneously in the same narrow frequency sub-band using SDMA. It is noteworthy that the BS will potentially serve K', K'' etc. users in the other sub-bands at the same time. However, in this study, we focus on the system simulations only in a single sub-band to analyse the SDMA performance in a single time-frequency resource block. Let $\boldsymbol{q}$ contain the symbols intended for the users ($E\{|q_k|^2\} = 1$), $\boldsymbol{\rho}$ contain user signal-to-noise ratios (SNRs), $\boldsymbol{n}$ consists of the unit-variance additive white Gaussian noise at each user and $\boldsymbol{y}$ be the received signal vector, such that $\{\boldsymbol{q}, \boldsymbol{\rho}, \boldsymbol{n}, \boldsymbol{y}\} \in \mathbb{C}^{Kx1}$.

The precoded signal vector $\boldsymbol{x} \in \mathbb{C}^{Mx1}$ is simply given by

$$\boldsymbol{x} = \boldsymbol{W}\boldsymbol{q} \tag{1}$$

where $\boldsymbol{W} \in \mathbb{C}^{MxK}$ is the precoding matrix satisfying

$$\sum_{m=1}^{M} |W_{m,k}|^2 = 1 \quad \text{for} \quad \forall k \in \{1, \ldots, K\} \tag{2}$$

Furthermore, the received signal vector $\boldsymbol{y}$ can be computed by

$$\boldsymbol{y} = \boldsymbol{\rho} \cdot (\boldsymbol{H}\boldsymbol{x}) + \boldsymbol{n} \tag{3}$$

where $\boldsymbol{H} \in \mathbb{C}^{KxM}$ denotes the downlink channel matrix with $E\{|H_{k,m}|^2\} = 1$ whose entries are formulated as [33]

$$H_{k,m} = \beta_{k,m} G_m(\hat{\boldsymbol{r}}_{km}) \frac{\mathrm{e}^{-\mathrm{j}\frac{2\pi}{\lambda}|\boldsymbol{r}_k - \boldsymbol{r}_m|}}{|\boldsymbol{r}_k - \boldsymbol{r}_m|} \tag{4}$$

where $G_m(\hat{\boldsymbol{r}}_{km})$ is the far-field function of the mth BS antenna element in the direction $\hat{\boldsymbol{r}}_{km}$ towards the kth user. $\beta_{k,m}$ is the normalisation constant.

Consequently, the SINR of the transmission from the BS array to the kth user is given by

$$\mathrm{SINR}_k = \frac{\rho_{k,k} \left|\boldsymbol{H}_{k,:}\boldsymbol{W}_{:,k}\right|^2}{\sum_{j \neq k}^{K} \rho_{k,j} \left|\boldsymbol{H}_{k,:}\boldsymbol{W}_{:,j}\right|^2 + 1} \tag{5}$$

where $\rho_{k,j}$ is the SNR at the kth user while serving the jth user, which is given by

$$\begin{aligned} \rho_{k,j}(\mathrm{dB}) = {} & P_j(\mathrm{dBm}) - 20\log_{10}[f_c] - 20\log_{10}\left[\frac{4\pi}{c}\right] \\ & - 20\log_{10}[|\boldsymbol{r}_k - \boldsymbol{r}_m|] + G_m(\hat{\boldsymbol{r}}_{km})(\mathrm{dB}) - N_{\mathrm{th}}(\mathrm{dBm}) \end{aligned} \tag{6}$$

where f_c is the carrier frequency, N_{th} is the thermal noise power, and P_j is the average adaptive transmit power to the jth user with equalised SNRs, which is calculated by

$$P_j = P_{max} \frac{(d^2_{user,\,j})}{\max\,(\boldsymbol{d}^2_{user})} \frac{\cos(\,\min\,(\boldsymbol{\theta}_{sc}))}{\cos(\theta_{sc,\,j})} \tag{7}$$

where $\boldsymbol{d}_{user}$ is a vector containing the distances between the users and the BS and $\boldsymbol{\theta}_{sc} \in \mathbb{C}^{Kx1}$ contains the scan angles towards the users.

Regarding the precoding algorithms, two commonly applied techniques, CB and ZF, are studied for which the precoding matrix $\boldsymbol{W}$ is given by

$$\boldsymbol{W} = \begin{cases} \boldsymbol{H}^{\dagger} & \text{for CB} \\ \boldsymbol{H}^{\dagger}(\boldsymbol{H}\boldsymbol{H}^{\dagger})^{-1} & \text{for ZF} \end{cases} \tag{8}$$

where † denotes the Hermitian transpose.

Table 3 List of sector simulation parameters

Parameter definition	Symbol	Value
centre frequency, GHz	f_c	28
number of antennas at the BS	M	64
maximum cell range, m	r_{max}	200
angular width of a sector in azimuth (deg.)	Φ_{sector}	±60
directivity of each antenna element at Tx, dB	$D_{tx,\,el}$	8
directivity of each user antenna at Rx, dB	D_{rx}	0
maximum average transmit power per user, dBm	P_{max}	26
bandwidth, MHz	BW	100
thermal power spectral density, dBm/Hz	PSD	−170
noise figure, dB	NF	10
thermal noise, dBm	N_{th}	−80
dissipated heat per chip per user, W	P_{diss}	0.5
number of random user location realisations	N_{sim}	10,000

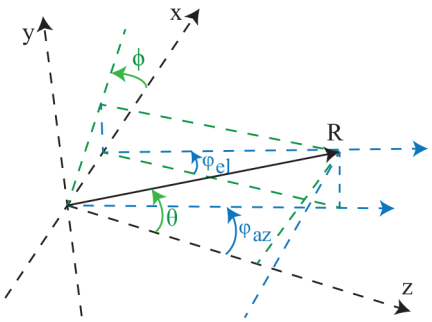

Fig. 2 *Coordinate system: conventional spherical coordinates and user elevation and azimuth angles*

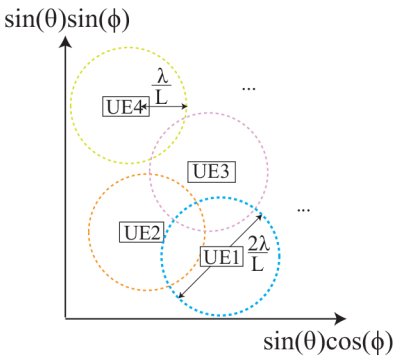

Fig. 3 *Visualisation of the interference-aware user selection (L represents the length of the antenna array)*

With an integrated link budget, Section 3 describes the LoS SDMA system model (C-i).

4 Use case scenarios

In this section, a generalised classification of the 5G mm-wave deployment scenarios is performed (C-ii). We consider two different use cases depending on the BS position and accordingly, the user locations (i.e. ground-only users and users/relays at different heights) with the common simulation parameters listed in Table 3. It is noteworthy that the two use cases investigated here represent the possible 5G mm-wave deployment scenarios that are currently discussed [34]. The ground-only user case mimics the scenario where the BS will be on a tower at a certain height, which does not require a large amount of vertical scanning range. The use case with users/relays at different heights, on the other hand, mimics the scenario where the BS is mounted lower to the ground, which will require vertical scanning ability to deliver signals across the buildings in elevation as well as to the users on the ground.

The coordinate system used in this study is shown in Fig. 2. The relation between the conventional spherical coordinate angles and the user elevation/azimuth angles is also provided in (9)

$$\begin{aligned} x = R\sin(\theta)\cos(\phi),\quad y = R\sin(\theta)\sin(\phi),\quad z = R\cos(\theta), \\ \varphi_{az} = \arctan(x/z) = \arctan(\tan(\theta)\cos(\phi)), \\ \varphi_{el} = \arctan(y/z) = \arctan(\tan(\theta)\sin(\phi)), \\ \phi = \arctan(\tan(\varphi_{el})/\tan(\varphi_{az})), \\ \theta = \arctan(\sqrt{\tan(\varphi_{el})^2 + \tan(\varphi_{az})^2}). \end{aligned} \tag{9}$$

To ensure high gain at each user and avoid very high interferences, we use an intuitive user selection algorithm (C-iii) based on forbidding the users to be inside each others main beams in the antenna uv-plane, which is visualised in Fig. 3.

Next, the two use cases with ground-only users and users/relays at different heights are explained in more detail.

4.1 Ground users

In this case, the users are uniformly distributed on the ground in the cell sector and it is assumed that the BS is located at a height of 10.5 m from the users. A sample distribution of locations for eight users is given in Fig. 4. After repeating the random user distribution for 10,000 times, a histogram of user elevation (φ_{el}) and azimuth (φ_{az}) angles is obtained, which is given in Fig. 5. It is seen that very small elevation angles below horizon occur the most, such that the number of occurrences starting from −3° at the cell edge up to −7° covers nearly 60% of the total occurrences. This is expected since most of the ground sector area can be covered by scanning φ_{el} by a few degrees, which makes the use of 2D scanning questionable for the ground-only users.

4.2 Users/relays at different heights

In this case, the sector is assumed to be formed by ±15° in elevation and ±60° in azimuth (which is used as the 5G cell definition in the current systems [35]) as shown in Fig. 6*a*. The users' locations are randomly picked from uniformly distributed points in the uv-plane using the interference-aware user selection algorithm. Moreover, the distances from each user to the BS are randomly picked from a scaled Beta distribution with $\alpha = 5$ and $\beta = 1$ in a range of [0, 200 m] to mimic the realistic scenario with higher probability for larger distances. The probability density function (PDF) of the Beta distribution used in this section is given in Fig. 7. Fig. 6 shows a sample selection of eight SDMA users in this case. Similar to the ground-only users, a statistical distribution of φ_{el} and φ_{az} for 10,000 random realisations is provided in Fig. 8, which shows more uniformity in the distribution of angles as compared to Fig. 5.

Note that according to Fig. 8, $|\varphi_{el}|$ can be larger than 15° (can reach up to 30° with low probability) and $|\varphi_{az}|$ can be slightly larger

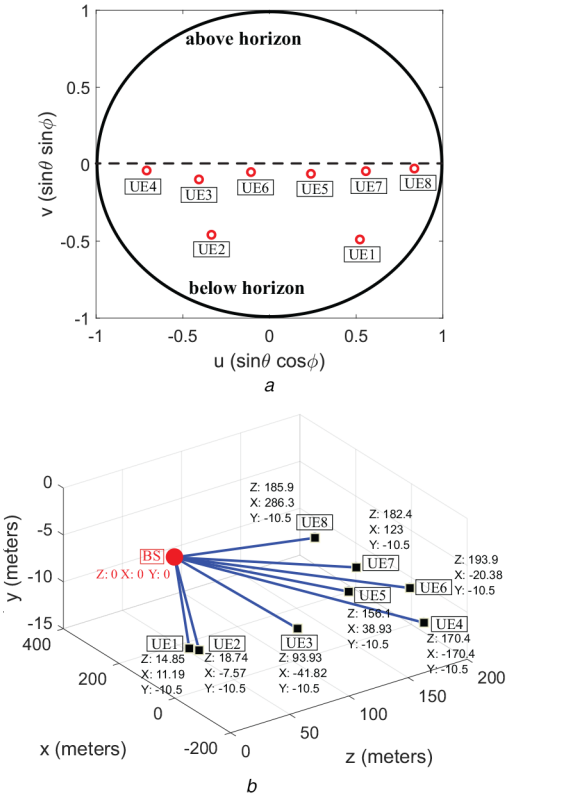

Fig. 4 *A sample distribution of eight random ground users with interference-aware selection in*
(a) *uv*-plane,
(b) Cartesian coordinates

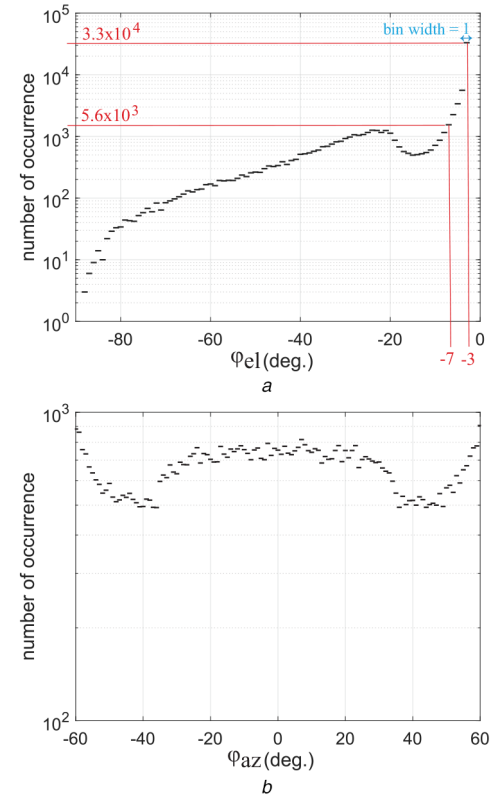

Fig. 5 *Statistical distribution of eight ground users with interference-aware selection for 10,000 random realisations*
(a) User elevation (φ_{el}),
(b) User azimuth (φ_{az})

than 60° (up to 64°), which is observed around the corners of the rectangular-shaped cell in the *uv*-plane.

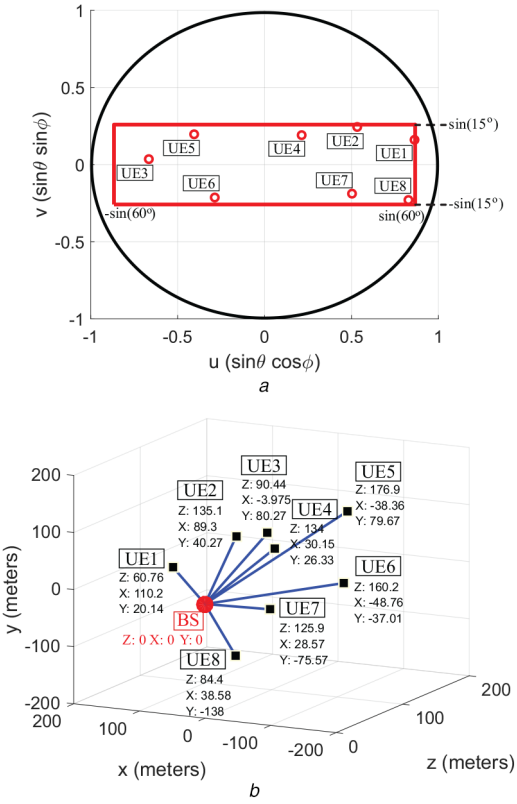

Fig. 6 *A sample distribution of eight random users/relays at different heights with interference-aware selection in*
(a) *uv*-plane,
(b) Cartesian coordinates

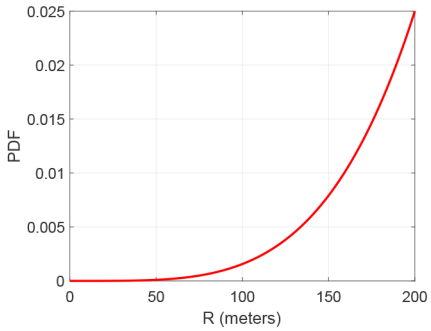

Fig. 7 *PDF of the Beta distribution with the design parameters* $\alpha = 5$ *and* $\beta = 1$*, scaled in an interval of* $R = [0, 200m]$

5 Simulation results

In this section, we investigate the QoS performance and computational complexities of the two beamforming techniques, namely CB and ZF, in MATLAB for the two use cases while using three different array topologies: the traditional, the 45° rotated, and the optimised (space-tapered) one (see Fig. 9). The optimised array is synthesised by using the convex element position perturbation technique in [20] (see Section 5.2 for more information).

5.1 CB using rotated arrays in use case A

In Fig. 5, it is seen that most of the users are located next to each other in the *uv*-plane at very small *v* values. In such a scenario, using the traditional array frequently results in having the high side lobes at the neighbouring users, as illustrated in Fig. 10*a*. However, by simply rotating the array by 45°, it is possible to shift the side lobes to the diagonal axis where, in most of the time, there are no users (see Fig. 10*b*). This analysis provides an original and intuitive approach to increase the statistical QoS via rotation of the traditional arrays placed on a square grid (C-iv).

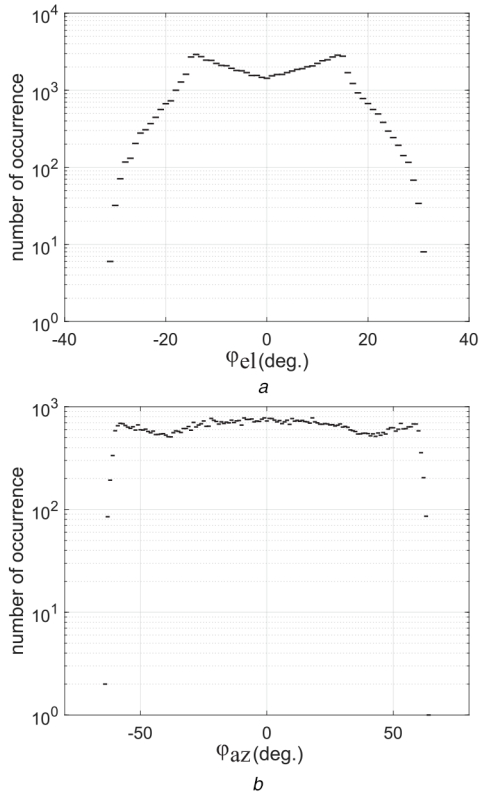

Fig. 8 *Statistical distribution of eight random users/relays at different heights with interference-aware selection for 10,000 random realisations*
(a) User elevation (φ_{el}),
(b) User azimuth (φ_{az})

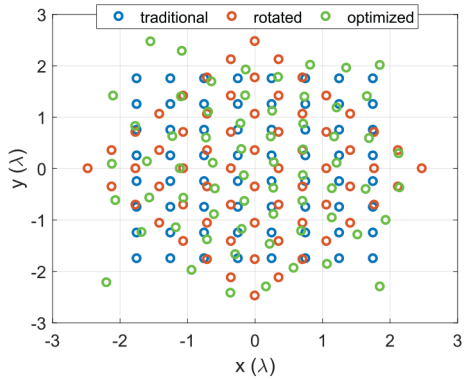

Fig. 9 *Investigated array layouts: traditional, rotated, and optimised arrays*

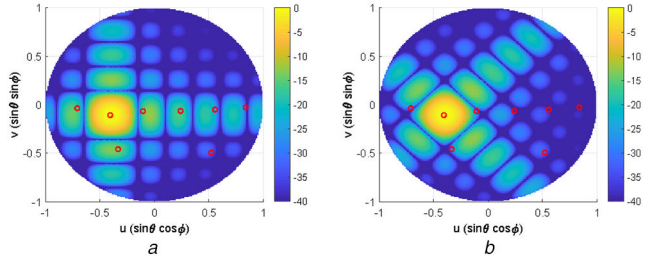

Fig. 10 *Normalised radiation patterns in use case A while serving UE3 in Fig. 4 with CB using*
(a) Traditional array,
(b) Rotated array

The QoS comparison for the two layouts is given in Fig. 11 for a different number of users in terms of CDF of SINR. In such graphs, it is a common practice to define a horizontal line at a certain CDF value that represents the percentage of occurrence (e.g. a line at a CDF value of 0.05 represents 95% of the cases).

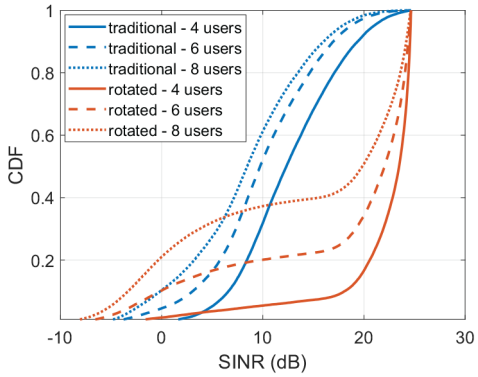

Fig. 11 *CDF of SINR in use case A using CB with the traditional and rotated arrays*

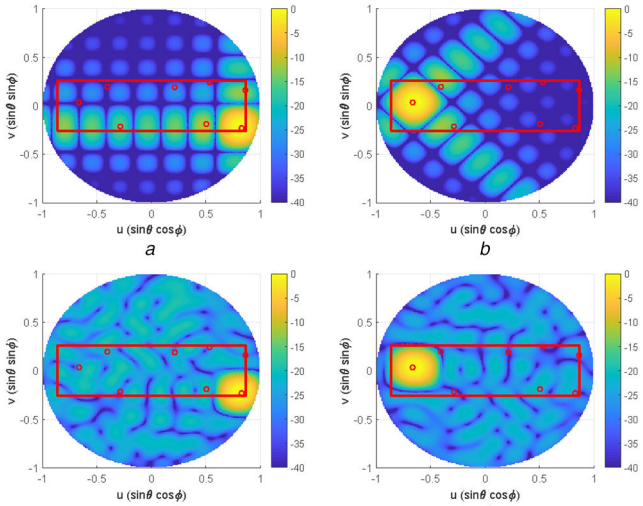

Fig. 12 *Normalised radiation patterns in use case B using CB and while serving a user in Fig. 6*
(a) UE8 with the traditional array,
(b) UE3 with the rotated array,
(c) UE8 with the optimised array,
(d) UE3 with the optimised array

The intersection point of this horizontal line with the related curve will give the minimum guaranteed SINR value for the chosen percentage of the total occurrences.

From Fig. 11, by looking at the intersection points as described, it is seen that the minimum guaranteed SINR becomes larger for the rotated array as compared to the traditional array when the pre-defined percentage of the total occurrences is < 97, 83 and 66% for $K = 4, 6$ and 8, respectively.

5.2 CB using space-tapered arrays in use case B

In Fig. 8, it is seen that in comparison with case A, the users are more uniformly distributed within the cell sector. In this case, it is expected that the optimised array layout with minimised SLL for a beam scanned towards any direction inside the cell sector (which is obtained using the convex element position perturbation technique in [20], an extension of the method in [19] to planar arrays) will statistically perform better than the traditional and rotated arrays. Therefore, in this section, we evaluate the statistical QoS performance of an optimised antenna layout (C-v), with minimum SLL for a pre-defined cell sector having 30°. and 120° angular width in elevation and azimuth, respectively.

The motivation for such a study is visualised in Fig. 12, where sample cases are shown supporting the reduced inter-user interference of the optimised array. As seen in Fig. 13, for the sector defined by $\pm 15°$ in elevation and $\pm 60°$ in azimuth, the max. SLL is reduced to -22 dB for the optimised array (note that it is around -13 dB for the traditional array, which is seen before the

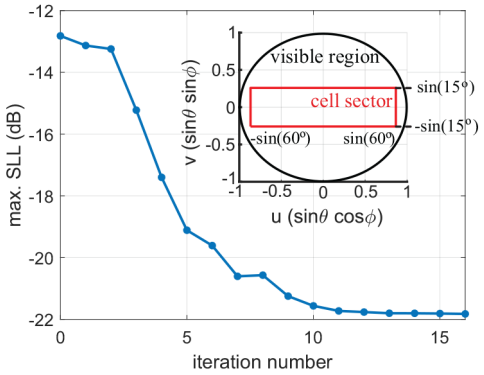

Fig. 13 *Iterative trend of the optimised array's max. SLL for multi-beam optimisation inside the cell sector, using the method in [20]*

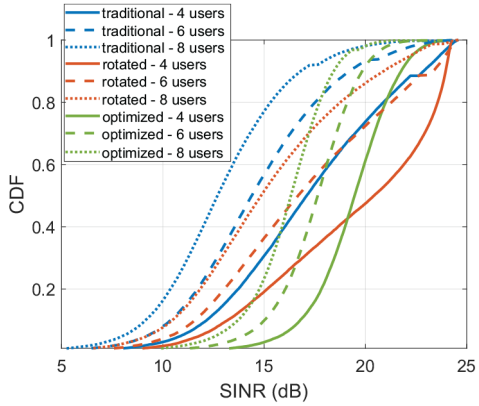

Fig. 14 *CDF of SINR in use case B using CB with the traditional, rotated, and optimised arrays*

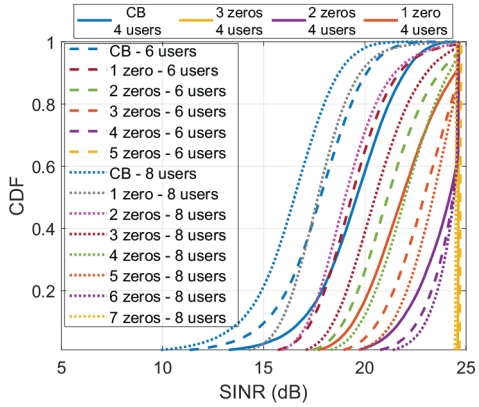

Fig. 15 *Reduced complexity ZF based on the number of zeros in use case B using the optimised array*

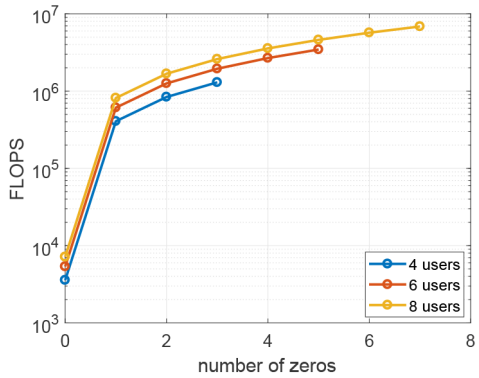

Fig. 16 *Computational complexity in reduced-complexity ZF (based on the number of zeros, with no zeros representing the CB) for a single realisation of the random user distribution*

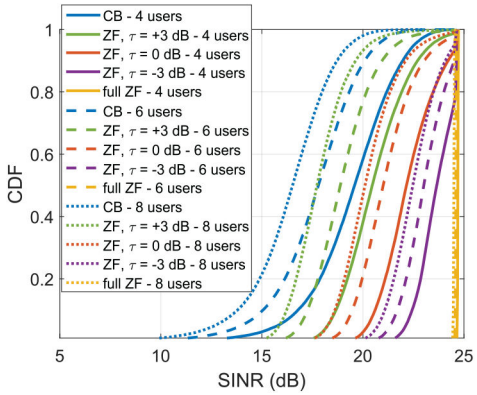

Fig. 17 *Reduced complexity ZF based on different INR threshold values (τ) in use case B using the optimised array*

first position perturbation, at iteration number 0 in Fig. 13). The CB results in this case, given in Fig. 14, shows that in 95% of the total occurrences, the minimum SINR is 4.9, 4.7 and 4.6 dB larger in the optimised array for $K = 4, 6$ and 8, respectively, as compared to the array with the traditional layout and 3.9, 3.6 and 3.4 dB larger for $K = 4, 6$ and 8, respectively, as compared the 45° rotated array.

5.3 ZF-ideal versus reduced complexity in use case B

ZF is superior to CB in terms of QoS since it can cancel out the interferences. However, the computational complexity of ZF is much larger than CB. Therefore, two different reduced complexity ZF algorithms are investigated here in use case B for the optimised array. Firstly, only the strongest N_c interferers are cancelled for each user as done in [10]. According to [10], the number of FLOPS in this case ($\#\mathcal{F}_{ZF}$) of ZF (for $N_c > 0$) is given by

$$\#\mathcal{F}_{ZF} = K(24N_cM^2 + 48N_c^2M + 54N_c^3 + 6M) \tag{10}$$

On the other hand, for CB (with no zeros), the number of FLOPS ($\#\mathcal{F}_{CB}$) is equal to

$$\#\mathcal{F}_{CB} = K(14M - 2) \tag{11}$$

SINR results for a different number of zeros per user (N_c) are given in Fig. 15. The number of FLOPS corresponding to different N_c and number of user (K) combinations is plotted in Fig. 16. It is seen that CB can provide a three-order of magnitude reduction in FLOPS as compared to the ideal ZF, but it has 8.8, 10.6 and 11.9 dB less minimum guaranteed SINR in 95% of the total occurrences for $K = 4, 6$, and 8, respectively. Therefore, reduced complexity ZF algorithm with a pre-defined N_c (depending on the SINR requirements) can provide a good compromise between the QoS and computational complexity (C-viii).

Secondly, instead of cancelling a constant number of interferers for each user, an adaptive cancellation scheme is proposed where the interferers whose power is larger than a certain threshold τ (with respect to the noise power) are cancelled out (C-vi and C-viii). The statistical SINR results in this approach for $\tau = +3$, 0 and -3 dB are given in Fig. 17.

6 Thermal aspects

In Table 3, the dissipated heat per chip per user is given as 0.5 W. Assuming fully-digital beamforming with one transceiver chip per antenna element and using the thermal modelling and design parameters indicated in [15] with a passive CPU cooler heat sink having a heat transfer coefficient of 3000 W/m^{2}K, we performed the thermal simulations in CST MWS for $K = 4, 6$, and 8 simultaneous, co-frequency users, leading to 2, 3 and 4 W dissipated heat per chip, respectively. The chip junction temperature results for the optimised array layout are given here in Fig. 18, which shows that the maximum temperature in the array

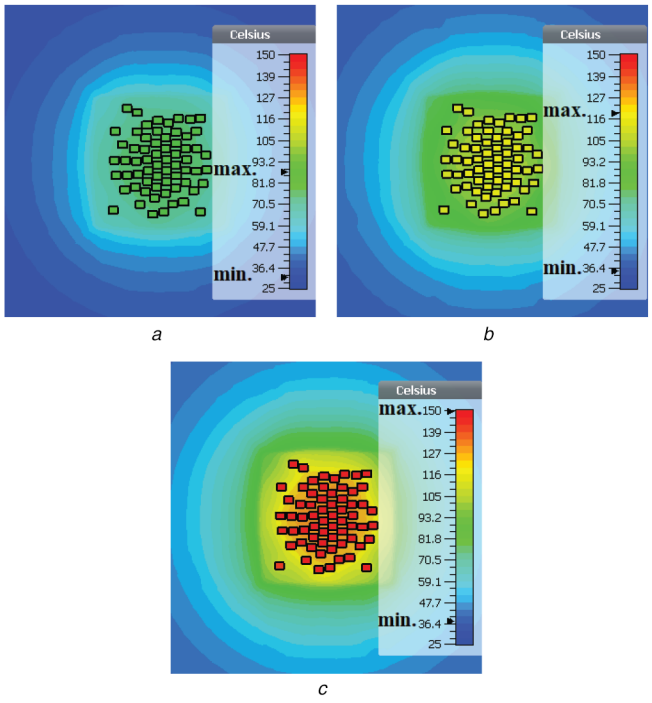

Fig. 18 *Maximum chip junction temperature in the passively cooled optimised array for*
(a) Four users,
(b) Six users,
(c) Eight users

increases from 85°C to 150°C when K is increased from 4 to 8. This clearly indicates the necessity to use more complex active cooling strategies (with fans or water pumps) for a large number of simultaneous users (C-vii).

7 Conclusion

Multiple complementary 5G research domains (interference-aware antenna layout synthesis, efficient front-end circuitry design, low-cost cooling, low-complexity signal processing, and MAC) are simultaneously addressed for the first time with the aim of evaluating the overall system performance of the mm-wave 5G BS antenna systems.

A multi-user SDMA model has been presented to investigate the trade-off between QoS, computational complexity, and cooling requirements for various use cases and a number of users with different beamforming algorithms and array layouts. A smart user selection method is used to ensure high gains at the intended user ends with a limited interference towards the other users and uniform-like power distribution across the array.

In the case of ground-only users, it has been seen that most of the users are located in the first few degrees in elevation below the horizon and simple rotation of the array can significantly increase the QoS with CB. For users/relays at different heights, on the other hand, optimised array layouts have been suggested to be used with CB due to their low average SLLs inside the cell sector.

ZF precoding has been observed to provide the best QoS (ideally with zero interference), but with the most computational complexity (three-order of magnitude larger than CB). Therefore, reduced complexity ZF algorithms (with up to an order of magnitude less complexity than the ideal ZF) have been proposed that are based on cancelling only a certain number of interferers for each user instead of all. It has been seen that such algorithms perform better than CB in terms of the statistical SINR even with the cancellation of only the strongest interferer, which exhibits a good compromise between the computational burden and QoS.

Furthermore, it has been shown that an increased number of simultaneous users and consequently, increased heat dissipation in the array raises the temperature above 100°C when using fully-passive cooling. This result shows a thermal-based limitation in the number of frequency re-use with a passively cooled system. To increase the number of simultaneous users above this limit, it is necessary to have a complex and high-cost active cooling system that requires energy and maintenance.

8 Acknowledgments

This research was conducted as part of the NWO-NXP Partnership Program on Advanced 5G Solutions within the project number 15590 entitled ‘Antenna Topologies and Frontend Configurations for Multiple Beam Generation’ and was funded in part by Netherlands Organisation for Scientific Research (NWO) and in part by NXP Semiconductors. More information: www.nwo.nl. The authors would like to thank Dr Ranga Rao Venkatesha Prasad for his valuable comments and assistance in preparing this paper.

9 References

[1] Ring, D.H.: ‘*Mobile telephony – wide area coverage – case 20564*’ (Bell Telephone Laboratories, New Jersey, United States, 1947)
[2] Magri, H., Abghour, N., Ouzzif, M.: ‘Key concepts of 5th generation mobile technology’, *WASET IJECE*, 2015, **9**, (4), pp. 471–474
[3] Odeh, N., Khatun, S., Ali, B.M., *et al.*: ‘Combined CDMA-SDMA performance analysis and code assignment algorithm’. Proc. IEEE Int. Conf. on Inventive Computation Technologies (ICICT), Dhaka, Bangladesh, March 2007
[4] Hong, W., Jiang, Z.H., Yu, C., *et al.*: ‘Multibeam antenna technologies for 5G wireless communications’, *IEEE Trans. Antennas Propag.*, 2017, **65**, (12), pp. 6231–6249
[5] Ali, E., Ismail, M., Nordin, R., *et al.*: ‘Beamforming techniques for massive MIMO systems in 5G: overview, classification, and trends for future research’, *Front. Inf. Technol. Electron. Eng.*, 2017, **18**, (6), pp. 753–772
[6] Rappaport, T.S., Xing, Y., MacCartney, G.R., *et al.*: ‘Overview of millimeter wave communications for fifth generation (5G) wireless networks with a focus on propagation models’, *IEEE Trans. Antennas Propag.*, 2017, **65**, (12), pp. 6213–6230
[7] Lebret, H., Boyd, S.: ‘Antenna pattern synthesis via convex optimization’, *IEEE Trans. Signal Process.*, 1997, **45**, (3), pp. 526–531
[8] Oraizi, H., Fallahpour, M.: ‘Nonuniformly spaced linear array design for the specified beamwidth/sidelobe level or specified directivity/sidelobe level with coupling considerations’, *Prog. Electromagn. Res. M*, 2008, **4**, pp. 185–209
[9] Bucci, O.M., D'Urso, M., Isernia, T., *et al.*: ‘Deterministic synthesis of uniform amplitude sparse arrays via new density taper techniques’, *IEEE Trans. Antennas Propag.*, 2010, **58**, (6), pp. 1949–1958
[10] Park, C.S., Byun, Y.S., Bokiye, A.M., *et al.*: ‘Complexity reduced zero-forcing beamforming in massive MIMO systems’. Proc. IEEE ITA Workshop, San Diego, CA, USA, February 2014
[11] Alkhateeb, A., Ayach, O.E., Leus, G., *et al.*: ‘Hybrid precoding for millimeter wave cellular systems with partial channel knowledge’. Proc. IEEE ITA Workshop, San Diego, CA, USA, February 2013
[12] Alkhateeb, A., Leus, G., Heath, R.W.: ‘Limited feedback hybrid precoding for multi-user millimeter wave systems’, *IEEE Trans. Wirel. Commun.*, 2015, **14**, (11), pp. 6481–6494
[13] Lee, B.M., Kim, Y.: ‘Zero forcing and codebook based beamforming scheme for practical usage of multiuser MIMO–OFDM with uplink channel sounding’, *Int. J. Commun. Syst.*, 2014, **30**, (1), pp. 6481–6494
[14] Khademi, S., DeCorte, E., Leus, G., *et al.*: ‘Convex optimization for joint zero-forcing and antenna selection in multiuser MISO systems’. Proc. 15th IEEE Signal Processing Advances in Wireless Communications (SPAWC), Toronto, ON, Canada, June 2014, pp. 30–34
[15] Aslan, Y., Puskely, J., Janssen, J.H.J., *et al.*: ‘Thermal-aware synthesis of 5G base station antenna arrays: an overview and a sparsity-based approach’, *IEEE Access*, 2018, **6**, pp. 58868–58882
[16] Kim, T., Park, J., Seol, J.Y., *et al.*: ‘Tens of gbps support with mmwave beamforming systems for next generation communications’. Proc. IEEE GLOBECOM 2013, Atlanta, GA, USA, December 2013
[17] Roh, W., Seol, J.Y., Park, J., *et al.*: ‘Millimeter-wave beamforming as an enabling technology for 5G cellular communications: theoretical feasibility and prototype results’, *IEEE Commun. Mag.*, 2014, **52**, (2), pp. 106–113
[18] Puskely, J., Aslan, Y., Roederer, A., *et al.*: ‘SIW based antenna array with power equalization in elevation plane for 5G base stations’. Proc. 12th European Conf. on Antennas and Propagation (EuCAP), London, UK, April 2018
[19] Aslan, Y., Puskely, J., Roederer, A., *et al.*: ‘Synthesis of multiple beam linear arrays with uniform amplitudes’. Proc. 12th European Conf. on Antennas and Propagation (EuCAP), London, UK, April 2018
[20] Aslan, Y., Puskely, J., Roederer, A., *et al.*: ‘Multiple beam synthesis of passively cooled 5G planar arrays using convex optimization’, *IEEE Trans. Antennas Propag.*, 2019, submitted for publication
[21] Aslan, Y., Puskely, J., Roederer, A., *et al.*: ‘Heat transfer enhancement in passively cooled 5G base station antennas using thick ground planes’. Proc. 13th European Conf. on Antennas and Propagation (EuCAP), Krakow, Poland, April 2019
[22] Sun, C., Ge, J., Li, J., *et al.*: ‘Low complexity user scheduling algorithm for energy-efficient multiuser multiple-input multiple-output systems’, *IET Commun.*, 2014, **8**, (3), pp. 343–350
[23] Chandra, K., Prasad, R.V., Niemegeers, I.G.M.M., *et al.*: ‘Adaptive beamwidth selection for contention based access periods in millimeter wave

WLANs'. Proc. 11th IEEE Consumer Communications and Networking Conf. (CCNC), Las Vegas, NV, USA, January 2014, pp. 458–464
[24] Chandra, K., Doff, A., Cao, Z., *et al.*: 'A 60 GHz MAC standardization: progress and way forward'. Proc. 12th IEEE Consumer Communications and Networking Conf. (CCNC), Las Vegas, NV, USA, January 2015, pp. 182–187
[25] Bencivenni, C., Glazunov, A.A., Maaskant, R., *et al.*: 'Effects of regular and aperiodic array layout in multi-user MIMO applications'. Proc. IEEE USNC/URSI NRSM, San Diego, CA, USA, July 2017
[26] Ge, X., Zi, R., Wang, H., *et al.*: 'Multi-user massive MIMO communication systems based on irregular antenna arrays', *IEEE Trans. Wireless Commun.*, 2016, **15**, (8), pp. 5287–5301
[27] Amani, N., Maaskant, R., Glazunov, A.A., *et al.*: 'Network model of a 5G MIMO base station antenna in a downlink multi-user scenario'. Proc. 12th European Conf. on Antennas and Propagation (EuCAP), London, UK, April 2018
[28] Degli-Esposti, V., Fuschini, F., Vitucci, E.M., *et al.*: 'Ray-tracing-based mm-wave beamforming assessment', *IEEE Access*, 2014, **2**, pp. 1314–1325
[29] Gottardi, G., Oliveri, G., Massa, A.: 'New antenna design concept for future generation wireless communication systems'. Proc. 12th European Conf. on Antennas and Propagation (EuCAP), London, UK, April 2018
[30] Wongchampa, P., Uthansakul, M.: 'Orthogonal beamforming for multiuser wireless communications: achieving higher received signal strength and throughput than with conventional beamforming', *IEEE Antennas Propag. Mag.*, 2017, **59**, (4), pp. 38–49
[31] Toso, G., Angeletti, P., Mangenot, C.: 'A comparison of density and amplitude tapering for transmit active arrays'. Proc. 3rd European Conf. on Antennas and Propagation (EuCAP), Berlin, Germany, March 2009
[32] Pi, Z., Khan, F.: 'An introduction to millimeter-wave mobile broadband systems', *IEEE Commun. Mag.*, 2011, **49**, (6), pp. 101–107
[33] Glazunov, A.A.: 'Impact of deficient array antenna elements on downlink massive MIMO performance in RIMP and random-LoS channels'. Proc. 12th European Conf. on Antennas and Propagation (EuCAP), London, UK, April 2018
[34] Cameron, T.: 'Bits to beams: RF technology evolution for 5G millimeter wave radios'. Tech. Art., Analog Devices Inc., 2018
[35] Degirmenci, E.: 'Emf test report: Ericsson AIR 5121'. Tech. Rep., GFTB-17:001589 Uen Rev B, Ericsson AB, Stockholm, Sweden, January 2018